Workshop on Virtual Reality Interaction and Physical Simulation VRIPHYS (2009)
H. Prautzsch, A. Schmitt, J. Bender, M. Teschner (Editors)

Soil Deformation Models for Real-Time Simulation: A Hybrid Approach

Daniel Holz, Thomas Beer, Torsten Kuhlen

Virtual Reality Group
RWTH Aachen University

Abstract

The simulation of soil deformation in real-time is a challenging task. Realizing the strengths and weaknesses of particle and mesh-based approaches we propose a hybrid model that combines both. Together with an adaptive sampling method, which effectively reduces the number of particles in the simulation, and a selective update technique our method is applicable in real-time VR environments. Furthermore, in order to account for the high degree of dynamics in soil behavior we consider soil as non-homogeneous and account for its degree of compaction. By incorporating soil mechanical formulations in our model and considering several physically plausible parameters the presented method allows for the simulation of soil as the material empirically investigated by civil engineers and soil mechanicians for decades.

Categories and Subject Descriptors (according to ACM CCS): I.3.7 [Computer Graphics]: Three-Dimensional Graphics and Realism—Virtual reality I.3.5 [Computer Graphics]: Computational Geometry and Object Modeling—Physically based modeling

1. Introduction

Soil exhibits a multitude of different behaviours depending on material properties, soil formations and interactions with the medium. The many phenomena of soil dynamics and their great impact can be observed in everyday life. When the foundation of roads or runways are prepared, soil compaction is used as a means to strengthen the soil in order to make it more resistant to stress. Moreover, during trenching in compacted soil, the side walls of the excavated trench remain stable even in rather steep slope formations, while the removed and dumped soil rests in a conical heap limited by a fixed angle, the soil's angle of repose α_r [LH93]. The reason for this is that the removed part enters a loosely packed state once escaping the confining pressure applied by the surrounding soil area, as opposed to the trench's side walls which remain in their initial compacted state. On the other hand, the same operation in dry, loose sand will result in immediate collapse of the side walls as soon as the angle of the sides exceeds a critical angle. After this small-scale avalanche the soil will come to rest in a formation which then again is subject to the angle of repose. The simulation of these dynamic phenomena is of great interest in the field of operator training. The demands of real-time simulator environments are rather high concerning both realistic visualization and physical correctness. Real life scenarios have to be displayed with sufficient accuracy. Therefore, in Virtual Reality (VR) training simulators for bulldozers, excavators but also planetary rovers a balance has to be found between interactivity and physical correctness of soil behavior. On one hand real-time performance is inevitable. On the other hand, also the highly dynamic effects of soil behavior have to be taken into account since this is what makes dealing with soil so challenging. Our main contributions are

- A new hybrid approach for the real-time simulation of soil deformations based on a particle- and grid-based representation of soil.
- The consideration of the soil's degree of compaction for the physically-plausible simulation of soil compaction and soil erosion.

After a brief overview of the recent developments in soil simulation in the following section, we will give some soil mechanics basics. Then we describe our proposed method, followed by a short outline of the applied real-time simu-

lation techniques. We conclude with the presentation of results, future work and give a conclusion.

2. Related work

In this section we will review a selection of works that address the problem of soil modeling in the field of Virtual Reality and Graphics. The approaches can be divided into mesh-based and particle-based methods.

Several of the mesh-based approaches use a heightfield data structure, not only for visual representation but also as underlying data structure of the soil simulated, one of which is [SOH99]. The authors present a soil propagation approach that is tailored to the animation of objects moving on ground. As in our approach, the deformable ground is modelled as rectangular soil columns represented by a uniform 2D grid. By detecting object ground intersections the amount of displaced ground is identified and propagated to the outside of the object's contour. Several non-physical parameters are provided that influence the appearance of the so-created mound of material in space and time, e.g. the mound's slope or the material's speed of propagation. A similar method is proposed by Onoue and Nishita in [ON03], who extend the approach in [SOH99] by representing both ground and objects by height spans, therefore allowing for some 3D effects. As in [SOH99] physical interaction between object and terrain is not taken into account. In the earlier work of Chanclou et al., [CLH96], the authors choose a physically plausible model. They consider loose soil as grains of sand in collision and use an ideal elasto-plastic model for its simulation. By linking point masses in a finite element fashion with plastic interactions even irreversible plastic deformations can be simulated. Additionally a refinement model is proposed to account for small-scale phenomena such as slipping of material. Also in [LM93] soil is considered as being subject to physical and mechanical laws. The authors Li et al. regard soil as a homogeneous medium and do not consider soil compaction. They choose a classical soil mechanics formulation, the Mohr-Coulomb criterion, as basis for their model. A 2D view of soil is discretized as an array of vertical slices where soil slippage occurs between two neighboring slices if shear stress exceeds soil strength along a possible failure plane. The exchange of soil matter on slippage is obtained locally for each pair of slices which leads to a linear equation system that describes the global flow of mass. The size of the system of equations depends on the number of soil slices simulated. By arranging 2D models in a hexagonal fashion the approach can be extended to 3D. The soil physical properties cohesion, and internal friction angle serve as parameters in the simulation. A 3D grid-based approach is presented in [RSJR09] for the simulation of bulk solids. The authors propose a 3D cellular automaton with each cell corresponding to a fixed volume of granular material. The method supports two-way coupling of bulk solids and rigid bodies.

We will begin the discussion of particle-based approaches with the work of Zhu and Bridson in [ZB05]. The authors combine and adapt the particle-based methods particle-in-cell (PIC) and fluid-implicit-particle (FLIP) to simulate sand in motion regarded as a fluid. By using a weighted average of the particle velocities obtained by both methods, PIC and FLIP, fine-grained parameterization of the material's viscosity is possible. The interaction of sand and water is addressed by the authors of [RSKN08], who use the Discrete Element Method (DEM) for the representation of granular particles and Smoothed Particle Hydrodynamics (SPH) for representing fluids. On collision between a granular and a fluid particle, the fluid particle is absorbed by the granular one and a so-called wetness value of the granular particle increases accordingly. The absorbed fluid is propagated between neighboring granular particles. In order to simulate the dynamics of wet granular material resulting from the formation of liquid bridges between solid grains, the amount of particle wetness is taken into account in the DEM part of the simulation. Also Bell et al. use a DEM approach to model the flow of granular material [BYM05]. They simulate angularity of granular particles by modelling a grain as a bulk of constrained spherical rigid bodies. In order to allow for granular material/rigid body interaction objects are covered with particles and included in the DEM simulation process. Bui et. al note the advantages of particle-based approaches over the conventional finite element method (FEM) when it comes to large soil deformation and failure [BFSW08]. They present the strength of their SPH-based elasto plastic soil model with the simulation of a slope failure scenario which includes interaction of soil with earth retaining structures.

Even though grids, especially heightfields, can be an efficient choice for soil simulation, because of the highly-plastic nature of soils, purely grid-based approaches are evidently not a good choice for their simulation. On the other hand, mesh-free methods like SPH or DEM are naturally well-suited when it comes to large displacements in a body. Unfortunately the strength of particle-based approaches to model both small-scale and large-scale phenomena comes with a weakness: the simulation of large deformable bodies requires a very high number of elements in order to achieve sufficient detail locally. This problem was addressed by Desbrun and Cani in [DC99], and Adams et al. in [APKG07]. Both works propose an adaptive sampling mechanism for particle-based fluid simulations with the goal to use a higher number of particles where necessary and to reduce the number of particles elsewhere.

3. Basics

In section 1 we mentioned the many effects of highly dynamic soil behavior and its impact on everyday life. How can we explain these phenomena? Soils consist of a soil skeleton formed by solid particles, e.g. quartz grains, and a considerable large part of voids, i.e. air and water. Thus, the total

volume of soil is defined as $V_T = V_S + V_V$ where V_S corresponds to the volume of solids and V_V to the volume of voids. When a given soil mass is subject to compressive stress, the soil grains approach and air and water are forced out of the soil skeleton, which decreases the ratio of volume of voids V_V to volume of solids V_S, called void ratio. The void ratio e is a measure for the compaction of soil and it is defined as $e = V_V / V_S$ where a lower void ratio corresponds to a higher compaction. The Mohr-Coulomb criterion describes the shear strength of soil, i.e. its resistence to shear stress, with given internal friction angle ϕ, cohesion c and under applied stress σ normal to the failure plane. Soil failure occurs if at some point the shear stress applied to the soil exceeds the shear strength. Therefore, this criterion can be applied to determine the slope angle at which a terrain formation becomes unstable and hence slips. It is given by

$$s = c + \sigma \tan\phi \tag{1}$$

with s denoting the soil's shear strength. The quantities s, σ and c have dimensions of force per unit area. The internal friction angle ϕ is a measure for the friction which acts inside a soil mass. As mentioned in [Das83] the angle of internal friction of granular soils is influenced by two factors which both contribute to its magnitude: the constant angle of sliding friction between the soil particles' surfaces, ϕ_μ, and the effect of particle interlocking, expressed as angle β, which increases with particle angularity. We obtain the formulation $\phi = \phi_\mu + \beta$ for the angle of internal friction. It is a known fact in the field of soil mechanics that the internal friction angle of granular soils is directly related to the packing of the particles, i.e. the degree of soil compaction. A denser packing, i.e. a more compact soil formation, yields higher internal friction. Since ϕ_μ is a constant, β must increase accordingly. In other words: the denser the packing, the higher the interlocking effect and hence, the more shear stress has to be applied to overcome this effect [Das83]. Note that in our model we ignore the small volume changes, called dilatency, as a result of the voids which emerge when the particles are lifted out of their locked positions. Returning to the Mohr-Coulomb criterion given in equation 1, we see that with higher soil compaction the shear strength of soil, s, increases due to a greater ϕ. When modeling terrain deformation, this highly dynamic behavior has to be accounted for. The compaction of soil itself can be observed, e.g., during traffic, which is a research interest in agricultural science. The area of terramechanics concentrates on investigating the behavior of wheeled or tracked vehicles performing on various types of soil surfaces [Won08]. In both fields, the effect of stress on the surface and its propagation in a soil mass are of interest. Various formulations exist that define stress distributions in soil subject to point loads, circular shaped loads or due to strip loads, so-called pressure bulbs [Won08].

Realizing the relation between degree of soil compaction and strength of soil and the resulting effects on soil behavior we see it as inevitable to consider soil as non-homogeneous material with different compaction degrees in the presented approach. We figured that maintaining and evolving the local compaction levels throughout the simulation is a requisite for simulating the dynamics of soil behavior described above.

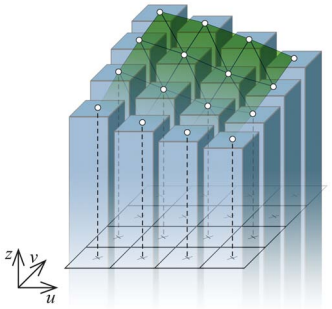

Figure 1: *Model of a continuous soil body as 2-dimensional array of rectangular soil columns and its visualization and data representation by a heightfield.*

4. Method

We propose a hybrid model for soil simulation which combines grid-based and particle-based methods, hence allowing us to take advantage of the strengths of both. Our approach is motivated by the occurrence of soil in nature: in equilibrium and not disturbed by outer forces soils remain in a static state, not showing any movement, while once exposed to a sufficiently high stress they show high plasticity. With a mesh-free particle-based approach the soil can evolve freely and unbound and therefore highly dynamic phenomena of soil behavior can be simulated. On the other hand choosing a heightfield as representation of soil in static state allows for fast collision detection and easy visualization. We consider the simulated soil as non-homogeneous by accounting for the soil's degree of compaction at each position.

In our approach we couple a heightfield for the representation of soil in its static state as in [SOH99], the *soil grid* representation, with a DEM-based simulation of soil in its loose, dynamic state, the *soil particle* representation. The soil grid is shown in figure 1. A continuous body of soil is approximated as an array of rectangular soil columns, each represented by a height value stored in a 2-dimensional grid structure. Note that we refer to the center located on top of such a soil column by the term *heightfield vertex*. The main idea of the presented model is to adaptively introduce deformability of a possibly large soil-covered area by replacing portions of the soil grid with soil particles. This enables the soil to displace freely in areas which undergo deformation. Once the soil particles settle and reach equilibrium, they will be merged back to the soil grid in a volume preserving manner. This greatly reduces the number of particles needed throughout the simulation and makes the method real-time capable.

We furthermore apply a physics-based adaptive soil sampling approach to reduce the number of particles in the simulation even more in order to meet the requirements of real-time applications. Since the method is intended for use in simulator environments where interaction between the soil and the rest of the scene is mandatory, we decided to base our simulation on a physics engine. This facilitates integration of the soil simulation module in an existing physics-based simulation since no particular care needs to be taken in order to realize the force exchange with other objects like machinery or humanoids. For implementation we chose the physics engine Vortex developed by CMLabs, which provides fast and accurate Newtonian physics simulation.

The method's framework architecture and its work flow is depicted in figure 2. The framework consists of a set of modules which together simulate the terrain in its different states of deformation. They are

- Soil particle generation (cf. section 4.1)
- Soil particle merging (cf. section 4.2)
- Soil grid compaction (cf. section 4.4)
- Soil grid erosion (cf. section 4.5).

For each rigid body colliding with the soil grid we perform *soil grid compaction* and *soil particle generation*. Information obtained from these stages are used to update a so-called *active vertices* list. This list serves for efficient processing in the *soil grid erosion* stage. Then soil particles in equilibrium are permanently merged with the soil grid by the *soil particle merging* module, which again updates the list of active vertices. Finally the *soil grid erosion* mechanism simulates propagation of soil in the soil grid caused by slip effects at unstable slopes.

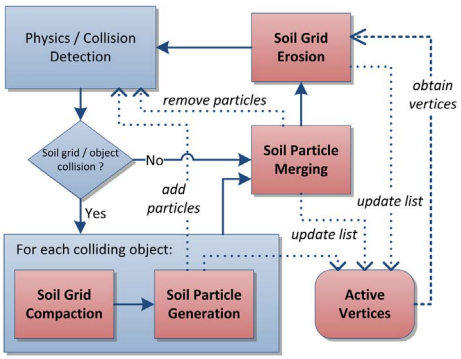

Figure 2: *Architecture and work flow of the proposed soil simulation framework.*

4.1. Soil particle generation

In order to simulate soil deformation on soil grid/tool interactions, e.g. a bucket digging or a wheel passing, we take a closer look at the area of contact, i.e. the vertices of the heightfield which intersect with the rigid body. We identify these by performing ray casts from below the terrain on all vertices which overlap or lie below the object's axis aligned bounding box and check for intersection. Deformation at these points might be due to soil failure for horizontal interaction and/or soil compaction for vertical interaction. Here we will discuss soil failure, simulated by the soil particle generation mechanism. We model soil failure by replacing a corresponding portion of the static soil column by soil particles and lowering the heightfield accordingly. For more details on the soil particle representation see section 4.3. Soil compaction yields the column to be lowered depending on the applied stress. See section 4.4 for more details. A basic approach would be to replace the part of the soil column which overlaps the object, identified as described. However, in the case of an object carving over the terrain, e.g. travelling from one grid vertex to a neighboring one, this technique is evidently subject to aliasing artifacts. If static soil were replaced by particles only as soon as object/soil column overlaps are detected the soil particle creation would depend on the object's speed, the timestep and the heightfield resolution. This might create sudden generation of a possibly large amount of particles as soon as the object reaches the next grid vertex, leading to physical and visual artifacts. We propose an anti-aliased carving method that operates velocity-based and identifies the area of soil that lies in front of the traveling object, e.g. the cutting blade. Ray casts along heightfield edges at the object's front are performed to identify the relative position of the front inbetween two neighboring heightfield vertices. Also an approximation of the object's deepest penetration point p under the front edge e is obtained by performing additional ray casts. We obtain the linear velocity of the object at p and derive its velocity v_d on the vertical plane which goes throug the edge. From these information we can compute the vertical velocity v_h with which we have to lower the heightfield vertex ahead such that the penetration point and the vertex reach a predetermined point s at the same time. This point is the section emerging from the tool's carving operation on the soil column which would appear if the tool's speed would remain constant. The equation describing this scenario is given as

$$t_d = t_h \Leftrightarrow d/v_d = h/v_h \tag{2}$$

with d and h denoting the distance to the section point s from the penetration point and the vertex respectively, and t_d, t_h being the time units necessary for traveling the corresponding distances. The soil column in front of the soil deforming object can hence be replaced by particles according to the height change Δh computed each frame which results in visually smooth deformations. The value of Δh can be obtained from $\Delta h = v_h \Delta t$ with Δt corresponding to the size of the timestep. The complete process is illustrated in figure 3.

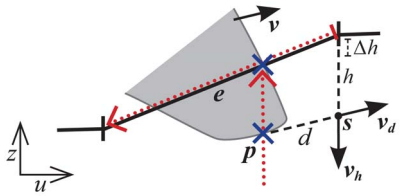

Figure 3: *Illustration of anti-aliased soil grid deformation. A rigid body (gray) yields displacement Δh of a heightfield vertex. Ray casts are depicted as dotted arrows.*

4.2. Soil particle merging

As soon as a soil particle in contact with the soil grid reaches a state of equilibrium, i.e. its angular and linear velocity values are smaller than a certain threshold value, its motion has no considerable impact anymore on the soil's dynamic. In this case, we remove it from the simulation and replace it with static volume in the soil grid by increasing the height of the corresponding soil column accordingly. We apply an interpolated filter kernel which guarantees volume preservation. More details on the applied kernel can be found in section 5.4. This approach considerably reduces the total number of particles in the simulation while not restricting the soil's dynamic behavior and therefore contributes significantly to the real-time capability of the method.

4.3. Soil particle representation

We simulate loose soil particles as spherical rigid bodies. As stated above we are currently using a physics engine for the particle dynamics. Therefore, the interaction between soil particles and other objects in the scene, e.g. the cutting blade of a bulldozer, are included in the physics engine's simulation loop. The material properties available in our simulation environment are the coefficient of sliding friction, cohesion/adhesion, stiffness and rolling friction for spherical rigid bodies. While the first three parameters are already provided by the physics engine, the latter one, rolling friction, is introduced manually. This measure is motivated by the results of Zhou et al., who showed that rolling friction plays an important role in molecular dynamics (MD) simulations of granular materials since it has a significant impact on the formation of stable heaps [ZWY*99]. We use a formulation for rolling friction on inter-particle contacts as presented in [ZWY*99] that simulates rolling friction as a torque M_i opposing particle i's current angular velocity ω_i. The applied contact model for the computation of M_i on interaction of particle i with particle j is depicted in figure 5 with the equation for M_i being

$$M_i = -\mu_r \left|V_{\omega,ij}\right| F_{cn,ij} \frac{\omega_i}{|\omega_i|} \tag{3}$$

where μ_r denotes the rolling friction coefficient and $F_{cn,ij}$ corresponds to the contact normal force. The term $\left|V_{\omega,ij}\right|$ describes the magnitude of relative linear velocity at the particles' contact point caused by the angular velocites ω_i and ω_j, which equals $|\omega_j \times R_j - \omega_i \times R_i|$. Here, the vectors R_i and R_j point to the contact point with origin in the center of particle i and j respectively. Their lengths equal the particles' radii.

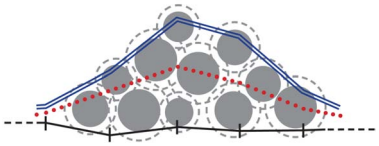

Figure 4: *Soil particles with solid and void parts (dashed) and surfaces resulting from merging with (double-stroke) and without (dots) consideration of voids.*

To achieve stable results in the simulation we take special care in limiting the torque applied, so as not to exceed the magnitude of the present angular velocity, which would create an unnatural flip of the direction of rotation. In this context we have to account for two scenarios, both of which could result in a too high torque: high normal forces in particle/particle and particle/object interactions on one hand, and accumulated rolling friction in one time step when it comes to multiple interactions with the same particle on the other hand. Our solution shows stable results that are visually comparable with the results in [ZWY*99] (cf. fig. 11).

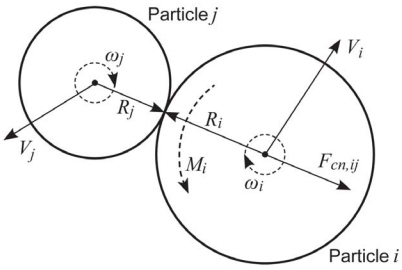

Figure 5: *Contact model as in [ZWY*99] used for the computation of rolling friction for particle i modelled as torque M_i.*

In the soil particle representation we account for the soil's compaction degree by assigning a void ratio value to free soil particles, which is updated in each simulation step. More details on how to obtain this measure are given in section 5.2. In this way soil can be represented as it appears in nature: Depending on the type of soil and its degree of compaction a considerable amount of the soil's overall volume is formed by voids rather than solids. By considering the void ratio at a soil particle's position we are able to transfer the total volume to the soil grid once the particle reaches equilibrium and is merged back to the grid (cf. section 4.2). As we will describe in section 5.4, this method has a big impact on the

visual representation of the simulated soil. If only the solid volume sampled by the soil particles would be considered when merging them with the soil grid a mound of ground material would appear much lower than in reality (cf. fig. 4).

4.4. Soil grid compaction

As mentioned earlier, compaction significantly changes soil strength properties. In the proposed model we do not only maintain a measure of the soil's compaction level at each location in terms of void ratio e, we furthermore simulate compaction caused by compressive stress. The soil's compaction degree, expressed as void ratio, is stored per heightfield vertex in a linked list. Each entry consists of a height and a void ratio representing one soil layer. A linked list is a natural choice for the representation of a soil's layered structure since the impact of deformation, e.g. due to digging, corresponds with the list's traversal: starting from the top, we move further down, with the depth in accordance to the range of deformation. There are two types of compaction effects supported by our method, corresponding to the two soil representations, which are compaction of loose particles and compaction of the static soil grid. While the former is implicitly covered by the DEM simulation, the latter needs special attention.

In [OHD99] a simplified compaction model is presented, that takes as input a soil profile, given as specific volume ν against depth, and computes the profile's compaction as an increase in specific volume resulting from a tire rolling on the surface. Note that specific volume and void ratio are related by the relationship $e = \nu - 1$. The model makes use of the cam clay theory which relates specific volume to applied stress for a given type of soil. So called critical state parameters describe a soil type's elasto-plastic behavior in terms of this theory. The stresses acting inside the soil below the wheel are obtained from Froehlich's modification of the Boussinesq equation for stress distribution.The results presented by the authors agree well with experimental data.

We incorporate this model in our simulation environment by computing the stresses acting inside a soil column caused by the vertical forces applied during a soil grid/rigid body interaction. Similar to [OHD99] we update the soil's profile, represented by a linked list of soil layers with entries for void ratio and height. We compute the force present at a position on the soil surface by interpolation, taking into account the forces acting at the heightfield/rigid body contacts which are obtained from the physics engine. We then make use of the stress distribution equations to derive the stress below this point, apply the above mentioned compaction model by computing the increase in compaction degree for each layer in terms of void ratio. The resultant non-reversible, plastic strain is approximated by comparing the initial and the resultant void ratio and updating the layer's height accordingly. Due to the fact that the intial compaction state, i.e. void ratio, in a soil column is taken into account during this process, compaction of an already compacted soil creates correspondingly smaller strains. This is one of the effects of a soil's compaction degree on its behavior, which is successfully simulated by the presented compaction mechanism.

4.5. Soil grid erosion

Besides soil deformation resulting from direct interaction of rigid bodies with the soil grid, there is another type of deformation in grid regions which are not directly in contact with objects. As soon as soil deformation by soil grid/tool interaction occurs at some point the previously untouched terrain in the immediate environment is candidate for soil slippage. The slipping of soil is a result of shear stress caused by the soil's own weight. The left side of figure 6 shows a soil slope configuration where soil slip occurs along a so-called soil-failure plane, with an angle of inclination α. This is due to the fact that the shear stress force τ' applied by the soil wedge with weight W is higher than the *shear strength force* s' that keeps the wedge from sliding. One way of simulating this scenario would be to replace the soil wedge by particles and let the system evolve freely. However, in order to avoid unnecessary computational overhead we decided to apply a soil erosion approach without particle generation. A slope stability simulation recognizes soil slip by examining the geometrical configuration of neighboring soil columns in our soil grid representation. The described algorithm is based on the work presented in [LM93], where the authors approach the simulation of soil slippage and manipulation by using the Mohr-Coulomb criterion given in equation 1. The factor of safety, F, gives a measure for the likelihood of soil slip for a slope configuration as shown on the left side of figure 6. It is defined as

$$F := \frac{s'}{\tau'} = \frac{c \cdot L + W\cos(\alpha) \cdot tan(\phi)}{W\sin(\alpha)}, \qquad (4)$$

where c denotes cohesion and ϕ internal friction angle for the given soil slope and L corresponds to the length of the failure plane. Both s' and τ' denote magnitudes of force. If for all possible failure planes in the slope the factor of safety is ≥ 1, i.e. strength force exceeds stress force, the slope is stable. On the other hand if there exists at least one failure plane in the soil formation for which we have $F \leq 1$, i.e. shear stress exceeds or equals shear strength, soil failure and therefore soil slip is inevitable. By defining the factor of safety as a function $F(\alpha)$, only depending on the failure plane's inclination to the horizon α, and by finding its local minimum for the physically meaningful range of $0 < \alpha < \alpha_{max}$, with α_{max} corresponding to the slope angle, one can decide whether soil slip occurs. That is if there exists an α_0 with $F'(\alpha_0) = 0$ and $F(\alpha_0) \leq 1$. Similar to the authors of [LM93] we obtain a formulation for $F(\alpha)$ that fits our grid representation and hence, enables us to examine our soil grid for soil slip between neighboring soil columns.

We additionally propose an extension motivated by the

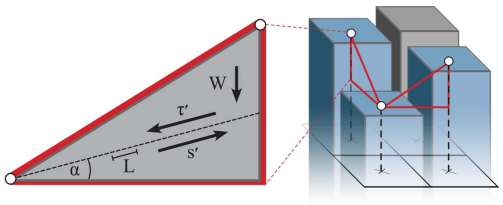

Figure 6: *Soil slope with failure plane (left) and local examination of soil grid for soil slip (right).*

observation described in section 3: a soil's shear strength is directly related to its degree of compaction. This means that the soil strength parameters, internal friction angle and cohesion, are no constants for a given type of soil but rather change with the soil's local compaction degree. Since these parameters directly influence the soil's local shear strength, as it can be seen in equation 1, they are significant for the soil's local slope stability, too. Soil slopes with different compaction show completely different erosion behaviour. We already gave an example from everyday life for this phenomenon in section 1. Trenching in a certain type of soil with low compaction might cause a collapse as soon as the trench walls exceed a particular angle while in the same soil with higher compaction the walls remain stable. The integration of this dynamic soil behavior is significant for a physically correct erosion simulation. Unfortunately, to the best of our knowledge, there are no known analytical formulations for the soil strength/compaction relationship. However, many experiments investigating this effect on many different soils have been conducted in the last decades which serve as an excellent source of data, e.g. [LW79]. Hence, we decided to incorporate this relation into the model as a look-up table that matches the soil's local compaction degree with its strength parameters. The table contains empirically obtained data points and linearly interpolates between them. With this data the degree of soil compaction of each slope formation can be taken into account when computing the soil slip that occurs from one frame to the next and the dynamic soil behavior described above can successfully be simulated. Note that there are several laboratory methods available for measuring the internal friction angles and cohesion magnitudes of a soil with different degrees of compaction, described in void ratio, e.g. the direct shear or the triaxial compression test [MHR96]. Once the inclination of the failure plane is determined, the evolution of the system, the soil erosion, can be computed by using an Euler integration scheme as described in detail in [LM93].

As opposed to the algorithm given in [LM93], which takes into account the exchange of soil mass between all neighboring soil columns in the complete grid at the same time and each frame, our method considers the soil slip of the soil simulated as a set of local problems. The authors of [LM93] state that both the incoming and outgoing soil mass for each soil column needs to be considered in order to guarantee volume preservation. They create one linear equation describing the soil flow per soil column and form a system of these linear equations which equals in size the total number of soil columns in the simulation, that can be solved by forward substitution. Hence, even if no soil slip occurred for some soil columns, computational time would still be spent on them during the simulation each frame. This is especially costly for large soil grids. Our solution is motivated by the fact that the biggest part of the terrain is in equilibrium and not subject to deformations, either by soil slip or soil/tool interactions. This means that a lot of computation time would be saved by simulating soil erosion only for those parts where it could actually occur. A simple technique reduces the problem of overall mass exchange by erosion to a set of local problems: for each soil column we take a look only at its right and upper neighbor, i.e. we examine the local slope configuration in positive u- and v-direction respectively, check each for soil slip and perform mass exchange if necessary (cf. figure 6 (right)). If we covered the complete soil grid with this local scheme the total soil flow by erosion would be considered. Of course, as mentioned above, the strength of this approach lies in the fact that we do not need to consider the complete grid but that we are able to resolve the soil erosion locally. Additionally the three dimensional problem of soil slip is reduced to two dimensions.The reader should note that a certain volume error is introduced that depends on the order of processing the soil columns and the timestep. However, with a sufficiently small timestep this error is negligible since the amount of soil mass transferred from one column to the other is very small, and therefore creates compared to the exact solution only small differences in soil flow which are visually not distinguishable. By construction of the scheme, the total volume is preserved nevertheless.

5. Real-time simulation techniques

We propose techniques and data structures for soil simulation which, first, are suitable for obtaining and storing the degree of soil compaction and, second, meet the requirements of simulating larger terrains in real-time.

5.1. Selective update

In order to efficiently simulate large terrains we address only those regions where actual deformation takes place locally. For this purpose we maintain a list of active heightfield vertices throughout the simulation, representing soil columns where soil deformation might occur. Figure 2 shows this list and its role in the method's work flow. This approach allows us to update the soil only where necessary and effectively avoids $O(n^2)$ time complexity for $n \times n$ heightfields. In case a soil grid/rigid body collision is detected the heightfield vertices which overlap the bounding box of the object are identified and flagged as active. Then the soil grid compaction and

soil particle generation is computed for each vertex independently, followed by the merging process. During this process all soil columns where actual merging occurred are flagged as active. The soil erosion module then processes only active vertices and removes vertices from the list where no filtering occurred. All processed vertices for which soil slip is performed are added to the list including their neighborhood. The list is reused in the next frame.

5.2. Spatial data structure

We apply a spatial data structure to obtain the void ratio at each soil particle's position using a particle-in-cell (PIC) approach [LL03]. When in equilibrium, the particle is merged with the heightfield and the particle's void ratio is used to decide whether a new soil layer is added or the top layer is updated. In particular the spatial data structure has to be capable of efficiently organizing soil particles which might be created everywhere on the terrain. In other words, the spatial extent of the data structure should only be limited by the size of the simulated terrain. We address this issue by proposing a 3D grid data structure, which has the general properties of a uniform 3D grid but is not limited by a given initial size. This is achieved by creating a grid of grids: actual uniform 3D grids are placed in space wherever necessary and managed in a hash grid structure. A hash function maps the three-dimensional coordinate (x,y,z), where $x,y,z \in \mathbb{Z}$, associated with a sub-grid and relative to the hash grid's origin to an integer value. It enables even perfect hashing in a fixed neighborhood of the origin, with the neighborhood's extend depending on the number of bits available to store the hash value. The flat hierarchical organization of this structure enables us to exploit both the strengths of uniform grids and hash grids: fast access times and good cache coherency for uniform grids and virtually unlimited spatial extent for hash grids. Furthermore, it allows for independent parallel hashing of the sub-grids.

5.3. Adaptive soil sampling

As mentioned earlier, we apply an adaptive soil sampling approach to reduce the number of particles in the simulation and, therefore, the time complexity. In case of a particle/particle collision their relative velocity at the contact point is examined. If a fixed threshold is not exceeded, i.e. the particles show strongly synchronized movement, the particles are locked in their relative positions and henceforth treated as one compound particle in the simulation loop. In order to maintain the particle's mass we compute the compound's inertia matrix from the old inertia matrices and test its sphericity, motivated by [DC99]. Here, the authors propose an error condition to test how close the shape of a set of particles is to a sphere based on their inertia matrix. Their method is based on an eigenvalue relationship but avoids an actual eigenvalue search to save computation time. We extend the condition by including a normalization step that allows us to obtain a general sphericity measure regardless of the object's mass. If the compound's shape deviates too much from spherical the merge is not performed since the compound particle would introduce a too high error. As soon as a sufficiently high force is applied to the compound particle, e.g. on impact, all the particles are split and, in this way, adaptively sample the soil under deformation.

5.4. Visualization

For visualization we blend particles which are directly on the terrain with the heightfield by applying a 1D binomial filter kernel in u- and v-direction (cf. fig. 1) respectively. This allows us to use the heightfield's geometry for the visualization of deforming terrain. Note that in contrast to the permanent merging mentioned in section 4.2, this merging process is solely graphical and does not change the rigid body representation of the soil grid in the physics engine. In order to address the aliasing artifacts that occur when particles travel from one vertex to the next, we compute an interpolated filter obtained from two different kernel sizes, and the particle's position relative to the closest heightfield vertex. Note that the interpolated kernel's partition of unity is preserved. This approach effectively eliminates the visual artifacts while guaranteeing volume preservation once the particle is permanently merged with the grid. Furthermore, the consideration of the particle's associated void ratio is of great importance during merging. Since a considerable part of a soil's overall volume consists of voids as described in section 3 their volume has to be accounted for. The total soil volume V_T, sampled by the particle, can be obtained by adding the particle's solid volume V_S, defined by its radius, to the void volume V_V, which can be derived from the particle's associated void ratio. The heightfield triangulation formed by merging the particles' total volume rather than only their solid volume with the soil grid gives a good approximation of the actual iso-surface of particles on the ground (cf. figure 4). This method gives a fast and simple solution for displaying particles in junction with the rest of the soil and yields good visual results.

In order to display the soil's particle flow we derive a velocity field from the topmost particles traveling on the ground and the soil erosion process which drives a texture coordinate-based flow visualization. We achieve a good visual representation of the particles' flow by blending an animated texture, showing a rather homogeneous granular material, with the actual heightfield texture. By avoiding the usage of a computationally expensive texture synthesis approach we save computation time for the simulation tasks which are more demanding.

6. Results

We show results of the method with a full physical data set for a sandy loam soil. The presented data was obtained on

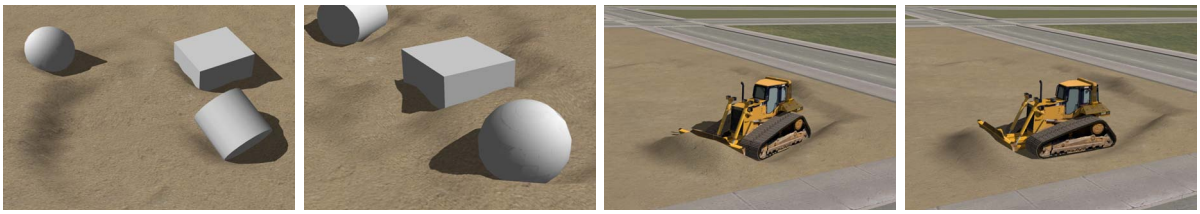

Figure 9: *Various objects and a bulldozer deforming a sandy loam soil.*

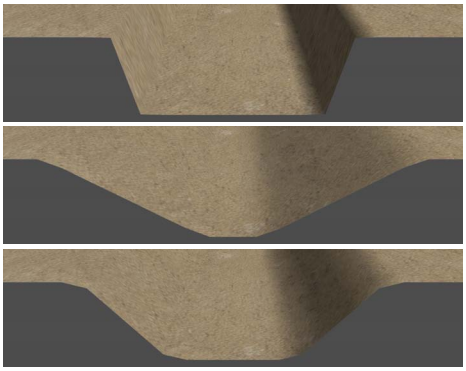

Figure 7: *Soil grid erosion: sandy loam soil trench (top) and resting state after collapse with initially low (middle) and medium (bottom) compaction degree.*

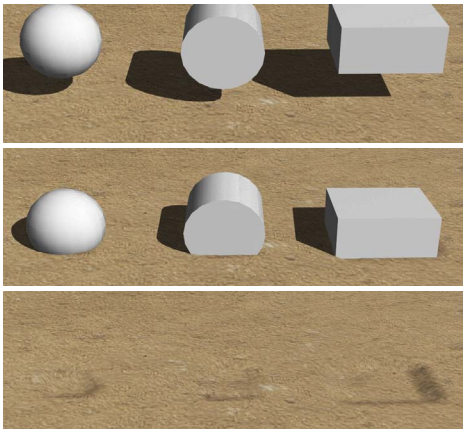

Figure 8: *Soil compaction caused by falling rigid bodies each having a mass of 2000 kg.*

a PC with Intel(R) Core(TM)2 Duo CPU at 1.8GHz, 4GB RAM and a NVIDIA Geforce 8600M GT graphics adapter. We demonstrate the dynamic behaviour of the soil grid erosion module by simulating the collapse of a trench with initially low and medium compaction degree. The results are shown in figure 7. In order to proof the physical correctness of the soil particle representation we extracted the angles of repose achieved in our simulation using a Hele-Shaw Cell which we reproduced in our simulation environment. Figures 9 and 8 show soil deformations of a sandy loam soil

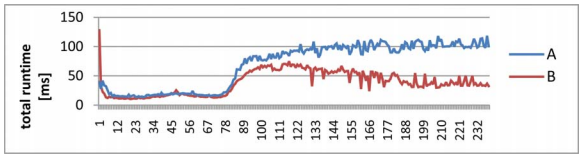

Figure 10: *Total simulation time in ms per frame used for 1000 soil particles falling into a box without (A) and with (B) adaptive soil sampling (cf. fig. 11).*

with low compaction degree caused by various rigid bodies. All objects except the bulldozer have equal mass of 2000 kg. The objects in figure 8 were dropped from a height of 5 meters. The average framerates for the most demanding interactions depicted in figure 9 were 103 fps for the left and 41 fps for the right pictures. The angle of repose is an emerging behaviour of soils directly related to several intrinsic soil parameters. Due to the abundance of research performed in this area and, therefore, the great wealth of experimental data, the angle of repose serves as a good candidate for validation. By appropriately setting the material properties for particle/particle contacts, i.e. cohesion, sliding and rolling friction, we were able to obtain angles ranging from 0° for saturated mud over 16° for clay to about 30° for dry sand. The angles were compared with values given in [Cai08]. We performed timing measurements for the adaptive soil sampling mechanism in a simulation of 1000 particles falling into a box. The results are given in figure 10. For the computationally expensive part starting at frame 90 we achieved a speed-up of almost 2. Figure 11 illustrates the similarity in physical behavior with (B) and without (A) adaptive soil sampling.

7. Future work and conclusion

Planned but not yet established is a physically correct soil failure model for the soil particle generation. The idea is to use one of the 2D cutting blade/soil interaction models known in soil mechanics independently in u- and v-direction. Our particle visualization approach does not consider particles which are seperate from the soil body. One

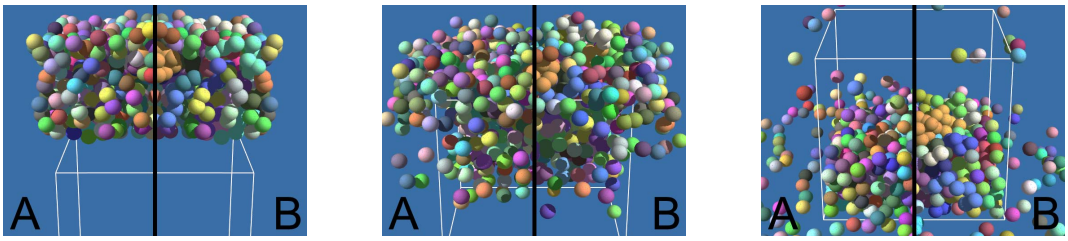

Figure 11: *1000 soil particles falling into a box without (A) and with (B) adaptive soil sampling. The pictures show frames 2, 50 and 160 from left to right. (A) shows mirrored version for comparison. In (B) merged particles are assigned the same color.*

possible solution would be a fast screen space iso-surfacing technique. However, since in real life soil particles appear in one connected body close to the ground most of the time, billboards would be an efficient and visually feasible alternative. In the future we would like to replace the 2.5D soil grid with a fully 3D data grid to allow for the method's application for the simulation of, e.g., mining scenarios. We are also investigating the simulation of particle interlocking and cohesion effects by applying our adaptive soil sampling technique for constraining compacted particles to one compound.

In this work we presented a method for the real-time simulation of deformable terrain. We provided for soil compaction by integrating a simplified but physically plausible compaction model and considered its result on dynamic soil behavior by linking a soil erosion mechanism with tables containing soil strength properties. We combined a particle-based and a mesh-based approach which enables highly plastic soil deformations while still permitting the method to operate in real-time. The method's architecture is designed in a modular way. The stages are independent and interchangeable and can therefore be replaced by more suitable mechanisms depending on the application's needs. This design approach would even allow to exchange the particle generation and simulation mechanism, e.g., for methods as presented in [ZB05] or [RSKN08] in order to simulate specific problems. An anti-aliased carving technique combined with anti-aliased kernel blending of particles with the ground allows for smooth soil/tool interactions. We furthermore presented real-time techniques which make efficient simulation and visualization even of large terrains feasible.

References

[APKG07] ADAMS B., PAULY M., KEISER R., GUIBAS L. J.: Adaptively sampled particle fluids. *ACM Trans. Graph. 26*, 3 (2007). 2

[BFSW08] BUI H. H., FUKAGAWA R., SAKO K., WELLS J. C.: Sph-based numerical simulations for large deformation of geomaterial considering soil-structure interaction. *IACMAG 1* (2008), 570–578. 2

[BYM05] BELL N., YU Y., MUCHA P. J.: Particle-based simulation of granular materials. In *SCA* (2005), pp. 77–86. 2

[Cai08] CAIN W.: *Earth Pressure: Retaining Walls and Bins*. Bibliobazaar, 2008. 9

[CLH96] CHANCLOU B., LUCIANI A., HABIBI A.: Physical models of loose soils dynamically marked by a moving object. *Computer Animation* (1996). 2

[Das83] DAS B. M.: *Advanced soil mechanics*. Hemisphere Publishing Corporation, 1983. 3

[DC99] DESBRUN M., CANI M.-P.: *Space-Time Adaptive Simulation of Highly Deformable Substances*. Tech. Rep. 3829, INRIA, 1999. 2, 8

[LH93] LEE J., HERRMANN H. J.: Angle of repose and angle of marginal stability: molecular dynamics of granular particles. *Journal of Physics A: Mathematical and General 26*, 2 (1993), 373–383. 1

[LL03] LIU G. R., LIU M. B.: *Smoothed Particle Hydrodynamics - A Meshfree Particle Method*. World Scientific, 2003. 8

[LM93] LI X., MOSHELL J. M.: Modeling soil: realtime dynamic models for soil slippage and manipulation. In *SIGGRAPH* (1993), pp. 361–368. 2, 6, 7

[LW79] LAMBE T., WHITMAN R.: *Soil mechanics*. Wiley, 1979. 7

[MHR96] MARSHALL T., HOLMES J., ROSE C.: *Soil Physics, third edition*. Cambridge University Press, 1996. 7

[OHD99] O'SULLIVAN M. F., HENSHALL J. K., DICKSON J. W.: A simplified method for estimating soil compaction. *Soil and Tillage Research 49*, 4 (1999), 325 – 335. 6

[ON03] ONOUE K., NISHITA T.: Virtual sandbox. *Computer Graphics and Applications* (2003), 252. 2

[RSJR09] ROSSMANN J., SCHLUSE M., JUNG T. J., RAST M.: Interaktive integrierte Starrkörperdynamik- und Schüttgutsimulation. In *ARVR* (2009), pp. 31–48. 2

[RSKN08] RUNGJIRATANANON W., SZEGO Z., KANAMORI Y., NISHITA T.: Real-time animation of sand-water interaction. *Computer Graphics Forum 27*, 7 (2008), 1887–1893. 2, 10

[SOH99] SUMNER R., O'BRIEN J. F., HODGINS J. K.: Animating sand, mud, and snow. *Computer Graphics Forum 18*, 1 (1999), 17–26. 2, 3

[Won08] WONG J.: *Theory of ground vehicles, fourth edition*. Wiley, 2008. 3

[ZB05] ZHU Y., BRIDSON R.: Animating sand as a fluid. In *SIGGRAPH* (2005), pp. 965–972. 2, 10

[ZWY*99] ZHOU Y. C., WRIGHT B. D., YANG R. Y., XU B. H., YU A. B.: Rolling friction in the dynamic simulation of sandpile formation. *Physica A: Statistical Mechanics and its Applications 269* (1999), 536–553. 5